Applied Physics Letters

# Spin orbit torque switching of magnetization in the presence of two different orthogonal spin–orbit magnetic fields

Cite as: Appl. Phys. Lett. **121**, 112403 (2022); https://doi.org/10.1063/5.0102200
Submitted: 08 June 2022 • Accepted: 23 August 2022 • Published Online: 13 September 2022

Seongjin Park, Kyung Jae Lee, Kyoul Han, et al.



## ARTICLES YOU MAY BE INTERESTED IN

Current-driven magnetization switching under zero field in Pt/Ta(wedge)/CoFeB/MgO multilayers
Applied Physics Letters **121**, 112407 (2022); https://doi.org/10.1063/5.0104427

Benchmarking of spin-orbit torque vs spin-transfer torque devices
Applied Physics Letters **121**, 112406 (2022); https://doi.org/10.1063/5.0101265

Enhancement of torque efficiency and spin Hall angle driven collaboratively by orbital torque and spin-orbit torque
Applied Physics Letters **121**, 072404 (2022); https://doi.org/10.1063/5.0086125



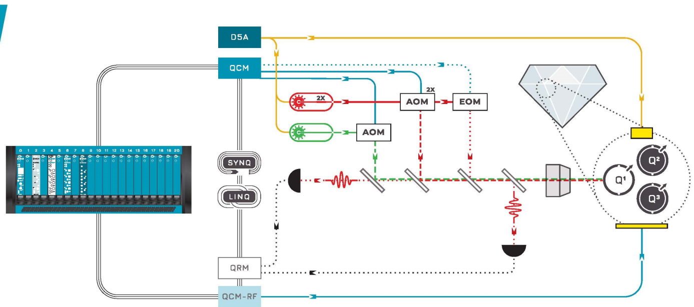

Applied Physics Letters ARTICLE scitation.org/journal/apl

# Spin orbit torque switching of magnetization in the presence of two different orthogonal spin–orbit magnetic fields

Cite as: Appl. Phys. Lett. **121**, 112403 (2022); doi: 10.1063/5.0102200
Submitted: 8 June 2022 · Accepted: 23 August 2022 ·
Published Online: 13 September 2022

View Online Export Citation CrossMark

Seongjin Park,[1] Kyung Jae Lee,[1] Kyoul Han,[1] Sanghoon Lee,[1,a)] Xinyu Liu,[2] Margaret Dobrowolska,[2] and Jacek K. Furdyna[2]

## AFFILIATIONS

[1]Physics Department, Korea University, Seoul 136-701, South Korea
[2]Physics Department, University of Notre Dame, Notre Dame, Indiana 46556, USA

[a)]Author to whom correspondence should be addressed: slee3@korea.ac.kr

## ABSTRACT

Switching of magnetization by spin–orbit torque in the (Ga,Mn)(As,P) film was studied with currents along ⟨100⟩ crystal directions and an in-plane magnetic field bias. This geometry allowed us to identify the presence of two independent spin–orbit-induced magnetic fields: the Rashba field and the Dresselhaus field. Specifically, we observe that when the in-plane bias field is along the current ($\mathbf{I} \parallel \mathbf{H}_{bias}$), switching is dominated by the Rashba field, while the Dresselhaus field dominates magnetization reversal when the bias field is perpendicular to the current ($\mathbf{I} \perp \mathbf{H}_{bias}$). In our experiments, the magnitudes of the Rashba and Dresselhaus fields were determined to be 2.0 and 7.5 Oe, respectively, at a current density of $8.0 \times 10^5$ A/cm$^2$.



Manipulation of magnetization by an applied current has received considerable attention during the last decade because of its relevance to the field of spintronics.[1–3] The most recent technique used for this purpose is spin–orbit torque (SOT) switching[4–7] in which spin-polarized charge carriers (i.e., spin current) exert a torque on local magnetization, reversing its sign. The spin polarization of current carriers can be achieved by various spin–orbit-related phenomena, including the Rashba[8,9] and Dresselhaus[10] effects, in crystals with inversion asymmetry, which are the subject of this paper. Importantly, the effect of inversion asymmetry in the crystalline material can be further enhanced by strain, which can be engineered by growing the film on a lattice-mismatched substrate.[11,12]

A unique feature of spin–orbit fields in zinc blende crystals occurs when the current flows along ⟨100⟩ crystallographic directions.[13] For such currents, the spin–orbit-induced (SOI) field due to the Rashba effect is perpendicular to the current, while the SOI fields arising from both the Dresselhaus effect and the strain are oriented along the current. Because the latter two SOI fields cannot be distinguished, we will refer to their joint effect as the Dresselhaus field. Currents flowing along the ⟨100⟩ directions, thus, provide a unique situation in which the Rashba and Dresselhaus SOI fields are orthogonal, causing orthogonal spin polarizations of charge carriers, thus allowing their effect to be experimentally distinguished. Investigation of magnetization switching by SOT in the presence of two orthogonal SOI fields, collinear and perpendicular to the current, may, thus, provide important insights for the manipulation of magnetization by current in strain-engineered crystalline FM structures. We note parenthetically that the presence of an SOI field collinear with the current offers the possibility for *field-free* magnetization switching by simultaneously using the Oersted field generated by a current pulse[14] because, in this case, the current-induced SOI field and the Oersted field are perpendicular to each other.

To study the effects of such coexisting orthogonal SOI fields in a strained crystalline ferromagnetic semiconductor film, we have chosen (Ga,Mn)(As,P), a ferromagnetic semiconductor with inversion asymmetry owing to its zinc blende structure.[13,15] By growing a (Ga,Mn)(As,P) layer on a GaAs substrate, we obtain films under tensile strain and, thus, with an out-of-plane magnetic easy axis.[16–21] In addition, structural inversion asymmetry presented at the interface of (Ga,Mn)(As,P)/GaAs contributes further to the Rashba effect.[22–24] In a (Ga,Mn)(As,P) film, directions of spin polarization collinear and perpendicular to the current can then be obtained via Dresselhaus and Rashba SOI fields when the current flows along ⟨100⟩ crystal directions, as shown in Fig. 1(a).

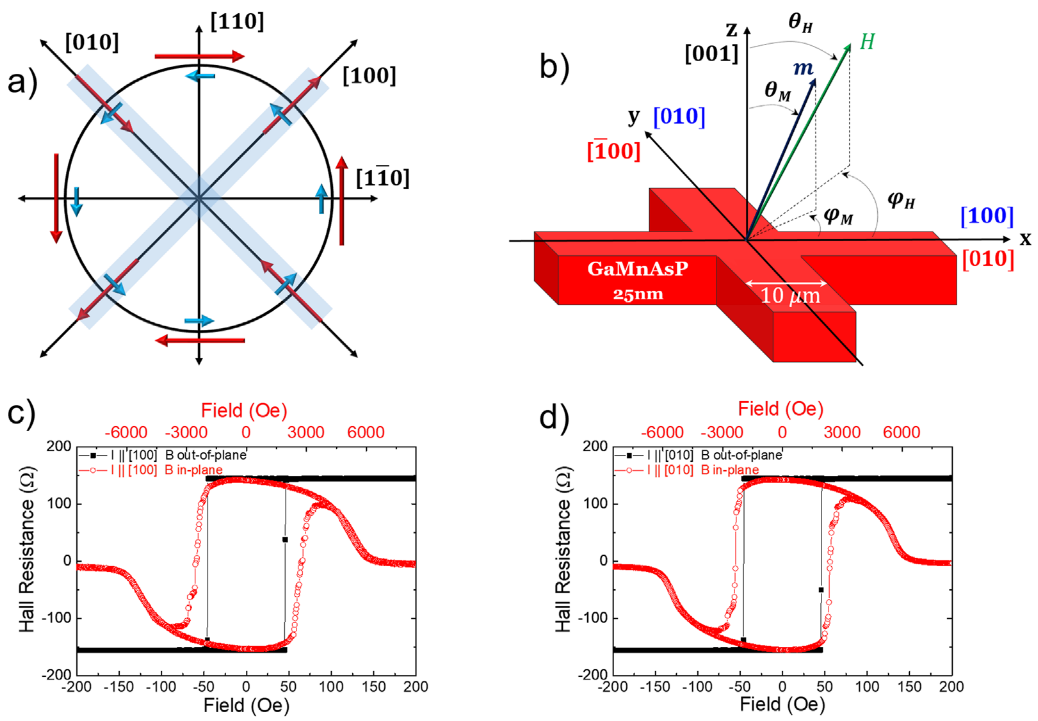


**FIG. 1.** (a) Directions of Rashba and Dresselhaus SOI fields (blue and red arrows, respectively) for current directions shown by thin black lines. Note that the two SOI fields are perpendicular to each other for currents along the ⟨100⟩ directions (marked with shaded regions). (b) Schematic diagram of our Hall bar device. The $x$ direction is defined by the direction of positive current, which can be either [100] or [010]. Panels (c) and (d) show Hall resistances observed on the (Ga,Mn)(As,P) film for out-of-plane ($\theta_H = 0°$) and in-plane ($\theta_H = 90°$, $\varphi_H = 90°$) field scans for currents along [100] and [010] directions, respectively. Hall resistance hystereses observed in [100] and [010] current directions are nearly identical, showing strong perpendicular magnetic anisotropy in the (Ga,Mn)(As,P) film.

For the present study, a 25 nm $Ga_{1-x}Mn_xAs_{1-y}P_y$ ferromagnetic layer was grown by molecular beam epitaxy (MBE) on a semi-insulating (001) GaAs substrate, with $x = 0.06$ and $y = 0.20$. In the growth, we used a substrate temperature of ~250 °C, known to be optimal for incorporating Mn into GaAs. For transport experiments, a $10 \times 10 \mu m^2$ crossbar Hall device was patterned by photolithography and dry etching, as shown schematically in Fig. 1(b), allowing us to study magnetization switching by SOT with currents along either [100] or [010] directions. Magnetization switching by SOT was monitored by measuring the anomalous Hall resistance (HR), which is proportional to the out-of-plane component of magnetization.

In this study, we define the $+x$ coordinate to be along the positive current, i.e., either along [100] or [010] direction, as shown in Fig. 1(b). The orientations of magnetic field and magnetization are indicated by angles $\theta_{H,M}$ and $\varphi_{H,M}$, respectively, where $\theta_{H,M}$ is measured from the $+z$ direction (i.e., from [001]) toward the film plane and $\varphi_{H,M}$ is measured counterclockwise (CCW) from the positive current direction (i.e., from $+x$ direction), as shown in Fig. 1(b). Hall resistance (HR) results measured at 55 K with a 100 $\mu$A current along [100] and [010] are shown in Figs. 1(c) and 1(d), respectively. The abruptness of HR transitions observed in the out-of-plane HR scans indicates a strong perpendicular anisotropy in the (Ga,Mn)(As,P) film.

HR measurements were performed at 55 K by scanning the current in the presence of an in-plane bias field $\mathbf{H}_{bias}$, using HR to monitor the SOT switching of magnetization. The HR results for currents in [100] and [010] directions are shown in Fig. 2. The data in Figs. 2(a)–2(d) are obtained with the current perpendicular to the in-plane bias field, $\mathbf{I} \perp \mathbf{H}_{bias}$, while those in Figs. 2(e)–2(h) are obtained in collinear measurement configuration, i.e., with current parallel or antiparallel to the bias field, $\mathbf{I} \parallel \mathbf{H}_{bias}$. For all measurements, the magnetization of the (Ga,Mn)(As,P) film was initially set either along the "up" direction ($\mathbf{M}_{ini} \parallel +z$, first row of Fig. 2) or along the "down" direction ($\mathbf{M}_{ini} \parallel -z$, second row) by a field of 2000 Oe applied along $\theta_H = 0°$ or $\theta_H = 180°$, respectively. Note that the observed switching behavior is quite different in the $\mathbf{I} \perp \mathbf{H}_{bias}$ configuration [Figs. 2(a)–2(d)] from that in $\mathbf{I} \parallel \mathbf{H}_{bias}$ [Figs. 2(e)–2(h)]. For example, the chirality of SOT switching observed for [100] and [010] current scans (indicated by dotted arrows in Fig. 2) is opposite for $\mathbf{I} \perp \mathbf{H}_{bias}$, while it is the same for $\mathbf{I} \parallel \mathbf{H}_{bias}$. In addition, the amplitude of the HR hysteresis is much larger in the $\mathbf{I} \perp \mathbf{H}_{bias}$ configuration than in $\mathbf{I} \parallel \mathbf{H}_{bias}$.

Since SOT switching is assisted by an external bias field, the amplitude of the HR hysteresis is expected to vary with external field strength. We have measured the dependence of SOT switching on the external bias field for the $I \parallel H_{bias}$ configuration, in which the maximum amplitude of HR hysteresis (i.e., maximum SOT switching ratio) was observed in the bias field region between 500 and 700 Oe (see the supplementary material, 1). As seen from Figs. 2(e)–2(h), the amplitude of the HR hysteresis for the $I \parallel H_{bias}$ configuration does not reach that observed for the $I \perp H_{bias}$ configuration, even with optimal bias field of 500 Oe. The switching ratio increases with bias field in the

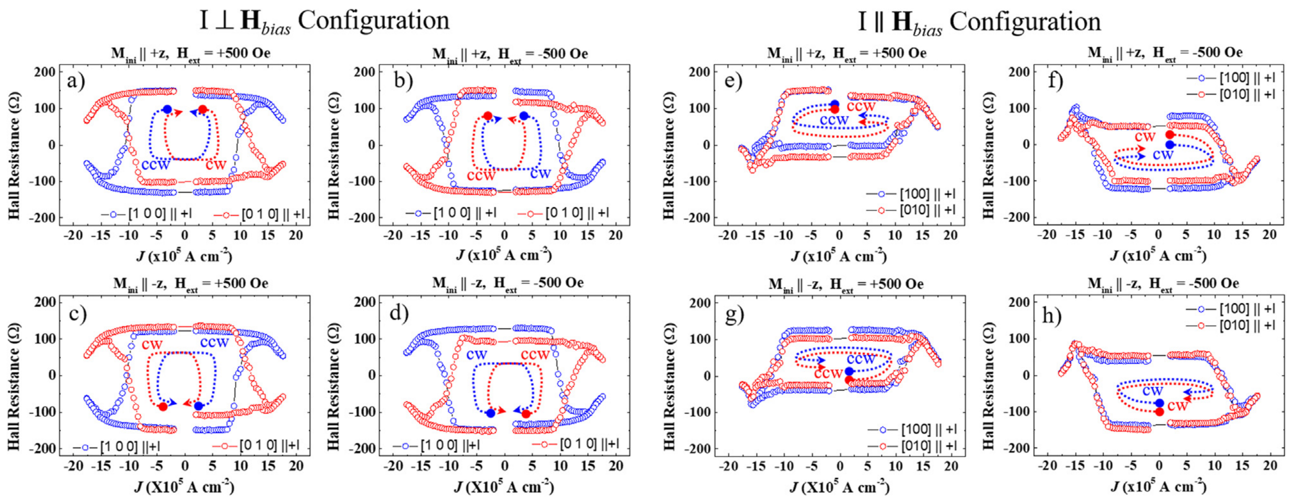


**FIG. 2.** SOT magnetization switching observed in the (Ga,Mn)(As,P) film during current scans. HR is measured as a function of current at 55 K for $\mathbf{I}\perp\mathbf{H}_{bias}$ (a)–(d) and $\mathbf{I}\parallel\mathbf{H}_{bias}$ (e)–(h). Initial conditions of magnetization direction and bias field used in the measurements are indicated in the panels, as is the order of the current scans followed in obtaining each hysteresis loop. Starting points of each scan are marked by blue and red solid circles.

region smaller than 500 Oe and then decreases with increasing bias in fields over 700 Oe (see the supplementary material, 1). A similar non-monotonic relation between the external bias field and switching current in SOT switching was observed on GaAs-based ferromagnetic semiconductor,[25,26] implying the involvement of some additional unrevealed mechanism in SOT switching of this material, which requires further investigation.

In order to understand the differences of SOT switching in the $\mathbf{I}\perp\mathbf{H}_{bias}$ and $\mathbf{I}\parallel\mathbf{H}_{bias}$ configurations, one needs to consider the joint effects of torques $\tau_{an}$, $\tau_{ext}$, and $\tau_{soi}$ caused, respectively, by the magnetic anisotropy field ($\boldsymbol{H}_{an}$), the external field ($\boldsymbol{H}_{ext}$), and the spin–orbit-induced fields ($\boldsymbol{H}_{soi}$). While the $\boldsymbol{H}_{an}$ and $\boldsymbol{H}_{ext}$ produce a torque given by the cross product to magnetization $\boldsymbol{M}$ and the field ($\tau_{an} = \boldsymbol{H}_{an}\times\boldsymbol{M}$ and $\tau_{ext} = \boldsymbol{H}_{ext}\times\boldsymbol{M}$), $\boldsymbol{H}_{soi}$ generates two types of SOT through spin polarization $\boldsymbol{\sigma}$ of current carriers: a field-like torque (FLT), given by $\boldsymbol{\sigma}\times\boldsymbol{M}$, and a damping-like torque (DLT), given by $\boldsymbol{M}\times(\boldsymbol{\sigma}\times\boldsymbol{M})$.[27] Earlier studies have shown, however, that in current-induced SOT magnetization switching in ferromagnetic films with an out-of-plane easy axis, DLT plays a dominant role,[14,25] and we will, therefore, restrict our attention to this process. Details of SOT switching for the [100] and [010] current directions are described in the supplementary material, 2.

For magnetization switching by SOT in ferromagnetic films with out-of-plane anisotropy, the symmetry between up and down magnetization states needs to be broken, as shown by Liu *et al.*[28] This condition can be achieved by an in-plane magnetic bias applied perpendicular to carrier spin polarization. In the case of ferromagnetic/heavy metal bilayers, where spin polarization is perpendicular to the current direction, an in-plane bias field collinear to the current (i.e., the $\mathbf{I}\parallel\mathbf{H}_{bias}$ configuration) is necessary.[29,30] The same requirement also applies to GaAs-based ferromagnetic semiconductor films with out-of-plane anisotropy when currents flow along $\langle 110\rangle$ directions, since in those configurations, both Dresselhaus and Rashba SOI fields are always perpendicular to the current [see Fig. 1(a)].[25,26] In contrast, for currents along $\langle 100\rangle$ directions in our present study, we observe SOT magnetization switching in *both* $\mathbf{I}\perp\mathbf{H}_{bias}$ and $\mathbf{I}\parallel\mathbf{H}_{bias}$ measurements, as was shown in Fig. 2. This implies the presence of two orthogonal components of carrier spin polarization for $\langle 100\rangle$-directed currents, as is, indeed, expected when both Dresselhaus and Rashba SOI fields are present [see Fig. 1(a)]. Furthermore, the analysis of these results indicates that the Dresselhaus SOI field plays the dominant role in switching magnetization in the $\mathbf{I}\perp\mathbf{H}_{bias}$ configuration, while switching in the $\mathbf{I}\parallel\mathbf{H}_{bias}$ case is primarily determined by the Rashba field, consistent with the requirement that, to achieve SOT switching, spin polarization and the in-plane bias field must be orthogonal. These relative roles of the Rashba and Dresselhaus fields are additionally confirmed by analyzing the sequence of magnetization switchings during the current scans in the $\mathbf{I}\parallel\mathbf{H}_{bias}$ and $\mathbf{I}\perp\mathbf{H}_{bias}$ geometries shown in Fig. 2 (i.e., the *chirality* of the process), as discussed in the supplementary material, 3.

The effect of SOT arising from current-induced SOI fields was also clearly observed in field scan measurements. The hysteresis of HR obtained with a current density of $8\times10^5$ A/cm$^2$ (2 mA) during in-plane field scans is shown in Fig. 3, where panels (a)–(d) and (e)–(h) are obtained, respectively, in the $\mathbf{I}\perp\mathbf{H}_{ext}$ and $\mathbf{I}\parallel\mathbf{H}_{ext}$ geometries. In Fig. 3, we refer to currents parallel to [100] or [010] directions as positive [plotted with black symbols in panels (a), (b), (e), and (f)], and to currents antiparallel to the [100] or [010] as negative [plotted with red symbols in panels (c), (d), (g), and (h)]. Data in Fig. 3 are significantly different from those obtained at a small current density of $4\times10^4$ A/cm$^2$, plotted in Figs. 1(c)–1(d), at which current-induced SOI fields are negligible. The complex shapes of hysteresis loops observed at the current density of $8\times10^5$ A/cm$^2$, showing multiple transition steps, are an indication of significant current-induced SOT effects caused by SOI fields during magnetization reversal.

A conspicuous feature of Fig. 3 is the strikingly different symmetry of hysteresis curves observed with opposite current polarities in $\mathbf{I}\perp\mathbf{H}_{ext}$ and $\mathbf{I}\parallel\mathbf{H}_{ext}$ configurations. In $\mathbf{I}\perp\mathbf{H}_{ext}$ measurements, where Dresselhaus SOI plays the dominant role, hysteresis for $+\mathbf{I}\parallel[100]$ and $-\mathbf{I}\parallel[010]$ has similar shapes [Figs. 3(a) and 3(d)], and so for

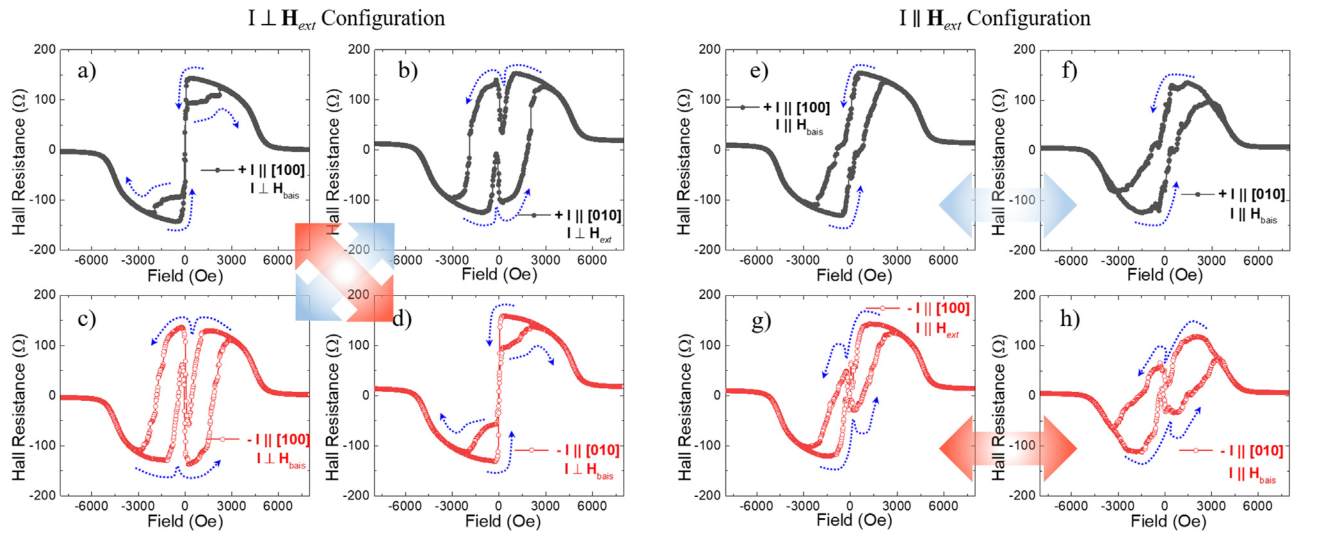


**FIG. 3.** HR hysteresis loops obtained by in-plane magnetic field scans at a current density of $8 \times 10^5$ A/cm$^2$ for the $\mathbf{I}\perp\mathbf{H}_{ext}$ (a)–(d) and $\mathbf{I}\,\|\,\mathbf{H}_{ext}$ (e)–(h) configurations. Thick arrows indicate similarities between hysteresis loops taken in various configurations and current directions. Dotted blue arrows show directions of field scans.

$-\mathbf{I}\,\|\,[100]$ and $+\mathbf{I}\,\|\,[010]$ [Figs. 3(b) and 3(c)]. These similarities and differences observed under different conditions match exactly the characteristics of the Dresselhaus field, which is parallel to the current in the [100] direction, but antiparallel when the current is in the [010] direction. In contrast, in the $\mathbf{I}\,\|\,\mathbf{H}_{ext}$ case, where SOT is dominated by the Rashba field, the hysteresis observed for $+\mathbf{I}\,\|\,[100]$ and $+\mathbf{I}\,\|\,[010]$ is similar [Figs. 3(e) and 3(f)], as for $-\mathbf{I}\,\|\,[100]$ and $-\mathbf{I}\,\|\,[010]$ [Figs. 3(g) and 3(h)]. This is consistent with characteristics of the Rashba field, whose direction is always at 90° measured CCW from the positive current direction. These similarities and differences among the hysteresis loops further support the fact that the dominant contribution to SOT switching in the $\mathbf{I}\perp\mathbf{H}_{ext}$ configuration comes from the Dresselhaus SOI field, while the Rashba field dominates in the $\mathbf{I}\,\|\,\mathbf{H}_{ext}$ configuration.

Having identified the respective roles of the Dresselhaus and Rashba SOI fields in magnetization switching by SOT through both current and field scan measurements, we can now determine the actual magnitudes of these fields. Even though second harmonic Hall voltage measurements are commonly used in studies of the SOT effect in FM/HM (heavy metal) systems,[31] this measurement technique is difficult to apply to GaAs-based ferromagnetics due to its relatively large thermal effects[14,32,33] (see the supplementary material, 4), which is detrimental to the second harmonic signal. We, therefore, use standard DC measurements for characterizing the SOI effective field in our GaMnAsP film. Since the direction of the SOI field is already confirmed by both the current and the field scan measurements (i.e., Figs. 2 and 3), this enabled us to use angle-dependent Hall measurements for the purpose of quantifying the magnitude of SOI fields. Since the magnitude of SOI fields for all ⟨100⟩ directions is the same, as already noted, we only focus on the configuration with the current along [010], as described below. The determination of SOI field can be done by measuring the angular dependences of HR for opposite current polarities as the applied field is rotated in the $x$–$z$ and $y$–$z$ planes. The difference $\Delta\theta$ of the field inclination $\theta_H$ at which magnetization switches observed in opposite current polarities then provides a direct measure of the SOI field, as given by the relation $H_{eff} = H_{ex} \cdot \Delta\theta$.[25,26,34]

The HR hysteresis loops observed with opposite currents along the [010] direction at a current density of $8 \times 10^5$ A/cm$^2$ (2 mA) are shown in Fig. 4. Figure 4(a) shows data obtained by rotating a field of 100 Oe clockwise (CW) in the $y$–$z$ plane [i.e., the (010) crystal plane], which is perpendicular to the current direction. This corresponds to the $\mathbf{I}\perp\mathbf{H}_{ext}$ configuration. Since the Dresselhaus SOI field dominates magnetization reversal in this configuration, the difference $\Delta\theta$ between the angles $\theta_H$ at which magnetization switches in the two current polarities in Fig. 4(a) provides a direct estimate of the Dresselhaus field. Figure 4(b), on the other hand, shows data observed by rotating the field in the $x$–$z$ plane [i.e., the (100) plane], which contains both the out-of-plane axis and the current direction. Since the Rashba field dominates SOT switching when the external field is collinear with the current (i.e., $\mathbf{I}\,\|\,\mathbf{H}_{ext}$ configuration), we can similarly estimate the Rashba field from $\Delta\theta$ observed with the two current polarities shown in Fig. 4(b). The Dresselhaus and Rashba SOI fields at a current density of $8.0 \times 10^5$ A/cm$^2$ obtained from the data in Fig. 4 are $H_{eff}^D = 7.5$ Oe and $H_{eff}^R = 2.0$ Oe, respectively. The $H_{eff}^D$ is about four times larger than $H_{eff}^R$, consistent with earlier estimates obtained in GaAs-based ferromagnetic semiconductor films.[26,35,36]

It is worth pointing out that this difference in the magnitudes of $H_{eff}^D$ and $H_{eff}^R$ is already reflected in Fig. 2. Note that the difference between the up and down magnetizations in the hysteresis curves shown in Fig. 2 is significantly smaller for the $\mathrm{I}\,\|\,\mathbf{H}_{bias}$ configuration than for $\mathrm{I}\perp\mathbf{H}_{bias}$. Here, it is important to realize that magnetically, the sample is actually a multidomain system, with pinning energies fluctuating from domain to domain as magnetization reverses. Thus, the stronger Dresselhaus field, which dominates magnetization switching in the $\mathrm{I}\perp\mathbf{H}_{bias}$ configuration, is able to reverse more domains than is the case with the weaker Rashba field in the $\mathbf{I}\,\|\,\mathbf{H}_{bias}$ geometry. This striking difference in the amplitude of the hysteresis observed in the $\mathbf{I}\perp\mathbf{H}_{bias}$ and $\mathbf{I}\,\|\,\mathbf{H}_{bias}$ data in Fig. 2, thus, provides additional evidence for the relative strengths of the two SOI fields.

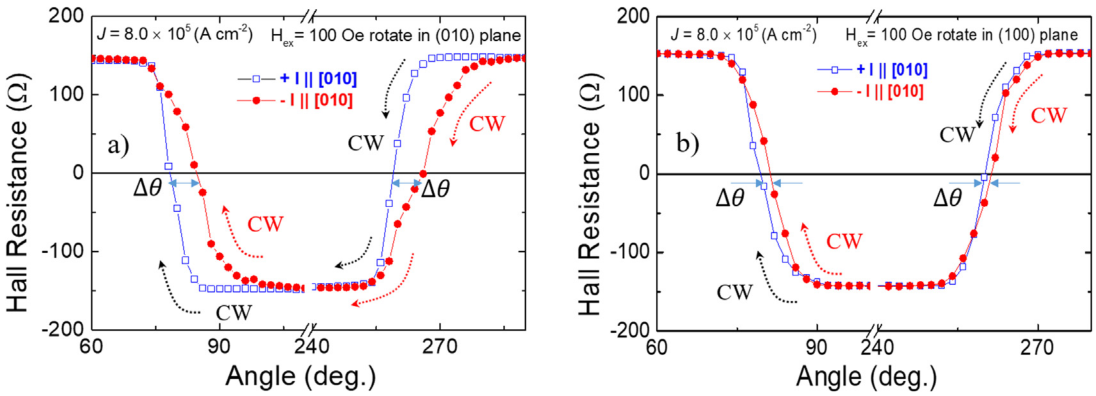


**FIG. 4.** Angular dependence of HR measured at a current density of $8.0 \times 10^5$ A/cm$^2$ in an external field of 100 Oe for positive and negative currents. Left panel shows data obtained with CW rotation of the external field in the plane perpendicular to the current [the *y–z* plane, i.e., the (010) crystal plane]. Right panel is obtained with the field rotated CW in the plane containing both the out-of-plane axis *z* and the current direction *x* [the *x–z* plane, i.e., the (100) plane]. Dotted arrows show CW sweep directions of the field. The difference in switching angles between the two current polarities is marked $\Delta\theta$, from which the magnitudes of $H^D_{eff}$ and $H^R_{eff}$ are obtained.

The results with current along the ⟨100⟩ crystallographic directions in the (Ga,Mn)(As,P) film in the presence of orthogonal SOI fields obtained in this work clearly demonstrate that SOT switching of perpendicular magnetization is possible in *both* $\mathbf{I} \perp \mathbf{H}_{bias}$ and $\mathbf{I} \parallel \mathbf{H}_{bias}$ configurations. The switching chirality of the current hysteresis loops in the $\mathbf{I} \perp \mathbf{H}_{bias}$ measurements was observed to be opposite for [100] and [010] current directions, indicating that the Dresselhaus-type SOI field plays the dominant role in SOT switching in that current configuration. In contrast, the SOT switching chirality of current hysteresis loops observed in the $\mathbf{I} \parallel \mathbf{H}_{bias}$ configuration was the same for currents flowing in [100] and [010] directions, which indicated that in that geometry, the Rashba-type SOI field played the major role in SOT switching. Importantly, the observation of SOT switching in the $\mathbf{I} \perp \mathbf{H}_{bias}$ geometry has special meaning for the case of field-free switching because the Oersted field around the current is always perpendicular to the current direction, which automatically satisfies the condition for SOT switching. If one strategically designs the GaAs-based ferromagnetic semiconductor (FMS) film specimens, such that the Oersted field is not canceled in the film, this will offer the possibility of *field-free* switching in which the role of $\mathbf{H}_{bias}$ can be replaced by the Oersted field generated by a current pulse, providing the opportunity for realizing extremely simple and energy efficient SOT devices based on a single ferromagnetic layer.

See the supplementary material for discussions about the switching chirality of current scan hysteresis and the dominant role of the Dresselhaus SOI field in SOT switching for $\mathbf{I} \perp \mathbf{H}_{\rm bias}$ configuration and of Rashba fields for $\mathbf{I} \parallel \mathbf{H}_{\rm bias}$.

This research was supported by the Basic Science Research Program through the National Research Foundation (NRF) of Korea (No. 2021R1A2C1003338), by the National Research Foundation of Korea (NRF) grant funded by the Korea government (MSIT) (No. 2022M3F3A2A03014536), by the NRF under the BK21 FOUR program at Korea University, Initiative for Science Frontiers on Upcoming Challenges, by the Korea University Grant, and by the National Science Foundation under Grant No. DMR 1905277.

## AUTHOR DECLARATIONS

### Conflict of Interest

The authors have no conflicts to disclose.

### Author Contributions

S.P. and K.J.L. contributed equally to this work.

**Seongjin Park:** Data curation (equal). **Kyung Jae Lee:** Data curation (equal). **Kyoul Han:** Data curation (equal). **Sanghoon Lee:** Conceptualization (equal); Supervision (equal); Writing – original draft (equal); Writing – review & editing (equal). **Xinyu Liu:** Resources (equal); Writing – review & editing (equal). **Margaret Dobrowolska:** Conceptualization (equal); Investigation (equal); Writing – review & editing (equal). **Jacek K. Furdyna:** Conceptualization (equal); Resources (equal); Writing – review & editing (equal).

## DATA AVAILABILITY

The data that support the findings of this study are available from the corresponding author upon reasonable request.

## REFERENCES

[1]J. C. Slonczewski, J. Magn. Magn. Mater. **159**(1), L1–L7 (1996).
[2]L. Berger, Phys. Rev. B **54**(13), 9353–9358 (1996).
[3]A. Brataas, A. D. Kent, and H. Ohno, Nat. Mater. **11**(5), 372–381 (2012).
[4]K. Garello, I. M. Miron, C. O. Avci, F. Freimuth, Y. Mokrousov, S. Blügel, S. Auffret, O. Boulle, G. Gaudin, and P. Gambardella, Nat. Nanotechnol. **8**(8), 587–593 (2013).
[5]I. Mihai Miron, G. Gaudin, S. Auffret, B. Rodmacq, A. Schuhl, S. Pizzini, J. Vogel, and P. Gambardella, Nat. Mater. **9**(3), 230–234 (2010).
[6]I. M. Miron, K. Garello, G. Gaudin, P.-J. Zermatten, M. V. Costache, S. Auffret, S. Bandiera, B. Rodmacq, A. Schuhl, and P. Gambardella, Nature **476**, 189–193 (2011).
[7]L. Liu, C.-F. Pai, Y. Li, H. W. Tseng, D. C. Ralph, and R. A. Buhrman, Science **336**, 555–558 (2012).
[8]Y. A. Bychkov and É. I. Rashba, JETP Lett. **39**(2), 78 (1984).
[9]K.-W. Kim, S.-M. Seo, J. Ryu, K.-J. Lee, and H.-W. Lee, Phys. Rev. B **85**(18), 180404 (2012).

[10]G. Dresselhaus, Phys. Rev. **100**(2), 580–586 (1955).
[11]Y. Kato, R. C. Myers, A. C. Gossard, and D. D. Awschalom, Nature **427**, 50–53 (2004).
[12]Y. K. Kato, R. C. Myers, A. C. Gossard, and D. D. Awschalom, Phys. Rev. Lett. **93**(17), 176601 (2004).
[13]B. A. Bernevig and S.-C. Zhang, Phys. Rev. B **72**(11), 115204 (2005).
[14]M. Jiang, H. Asahara, S. Sato, S. Ohya, and M. Tanaka, Nat. Electron. **3**(12), 751–756 (2020).
[15]S. D. Ganichev and L. E. Golub, Phys. Status Solidi B **251**(9), 1801–1823 (2014).
[16]M. Cubukcu, H. J. von Bardeleben, K. Khazen, J. L. Cantin, O. Mauguin, L. Largeau, and A. Lemaître, Phys. Rev. B **81**(4), 041202 (2010).
[17]M. Kopecký, J. Kub, F. Máca, J. Mašek, O. Pacherová, A. W. Rushforth, B. L. Gallagher, R. P. Campion, V. Novák, and T. Jungwirth, Phys. Rev. B **83**(23), 235324 (2011).
[18]H. Lee, J. Chang, P. Chongthanaphisut, S. Lee, S. Choi, S.-K. Bac, A. R. Nasir, S. Lee, A. Pardo, S. Dong, X. Li, X. Liu, J. K. Furdyna, and M. Dobrowolska, AIP Adv. **7**(5), 055809 (2017).
[19]A. Lemaître, A. Miard, L. Travers, O. Mauguin, L. Largeau, C. Gourdon, V. Jeudy, M. Tran, and J. M. George, Appl. Phys. Lett. **93**(2), 021123 (2008).
[20]A. W. Rushforth, M. Wang, N. R. S. Farley, R. P. Campion, K. W. Edmonds, C. R. Staddon, C. T. Foxon, and B. L. Gallagher, J. Appl. Phys. **104**(7), 073908 (2008).
[21]P. R. Stone, J. W. Beeman, K. M. Yu, and O. D. Dubon, Physica B **401–402**, 454–457 (2007).
[22]M. A. T. Sandoval, A. F. da Silva, E. A. de Andrada e Silva, and G. C. La Rocca, Phys. Procedia **28**, 95–98 (2012).
[23]Y. H. Park, H.-j. Kim, J. Chang, S. Hee Han, J. Eom, H.-J. Choi, and H. Cheol Koo, Appl. Phys. Lett. **103**(25), 252407 (2013).
[24]S. Gelfert, C. Frankerl, C. Reichl, D. Schuh, G. Salis, W. Wegscheider, D. Bougeard, T. Korn, and C. Schüller, Phys. Rev. B **101**(3), 035427 (2020).
[25]M. Jiang, H. Asahara, S. Sato, T. Kanaki, H. Yamasaki, S. Ohya, and M. Tanaka, Nat. Commun. **10**(1), 2590 (2019).
[26]S. Park, K. J. Lee, S. Lee, X. Liu, M. Dobrowolska, and J. K. Furdyna, APL Mater. **9**(10), 101102 (2021).
[27]C. O. Avci, K. Garello, C. Nistor, S. Godey, B. Ballesteros, A. Mugarza, A. Barla, M. Valvidares, E. Pellegrin, A. Ghosh, I. M. Miron, O. Boulle, S. Auffret, G. Gaudin, and P. Gambardella, Phys. Rev. B **89**(21), 214419 (2014).
[28]L. Liu, O. J. Lee, T. J. Gudmundsen, D. C. Ralph, and R. A. Buhrman, Phys. Rev. Lett. **109**(9), 096602 (2012).
[29]S. Fukami, T. Anekawa, C. Zhang, and H. Ohno, Nat. Nanotechnol. **11**(7), 621–625 (2016).
[30]Y. Yang, H. Xie, Y. Xu, Z. Luo, and Y. Wu, Phys. Rev. Appl. **13**(3), 034072 (2020).
[31]M. Hayashi, J. Kim, M. Yamanouchi, and H. Ohno, Phys. Rev. B **89**(14), 144425 (2014).
[32]S. Lee, T. Yoo, S.-K. Bac, S. Choi, H. Lee, S. Lee, X. Liu, M. Dobrowolska, and J. K. Furdyna, Sci. Rep. **7**(1), 10162 (2017).
[33]S. Lee, S. Lee, S. Bac, S. Choi, X. Liu, M. Dobrowolska, and J. K. Furdyna, IEEE Trans. Magn. **55**(2), 2400206 (2019).
[34]P. X. Zhang, L. Y. Liao, G. Y. Shi, R. Q. Zhang, H. Q. Wu, Y. Y. Wang, F. Pan, and C. Song, Phys. Rev. B **97**(21), 214403 (2018).
[35]A. Chernyshov, M. Overby, X. Liu, J. K. Furdyna, Y. Lyanda-Geller, and L. P. Rokhinson, Nat. Phys. **5**(9), 656–659 (2009).
[36]M. Endo, F. Matsukura, and H. Ohno, Appl. Phys. Lett. **97**(22), 222501 (2010).